Physiologia Plantarum

ORIGINAL RESEARCH OPEN ACCESS

L-Glutamine Modulates Root Architecture and Hormonal Balance in Arabidopsis

Barbora Pařízková[1] | Annika I. Johansson[2] | Marta Juvany[1] | Jan Šimura[1] | Karin Ljung[1] | Ioanna Antoniadi[1]

[1]Umeå Plant Science Centre, Department of Forest Genetics and Plant Physiology, Swedish University of Agricultural Sciences, Umeå, Sweden | [2]Umeå Plant Science Centre, Department of Plant Physiology, Umeå University, Umeå, Sweden

Correspondence: Karin Ljung (karin.ljung@slu.se) | Ioanna Antoniadi (ioanna.antoniadi@slu.se)

Received: 31 March 2025 | **Revised:** 11 December 2025 | **Accepted:** 15 December 2025

Handling Editor: C. Bellini

Keywords: auxin | cytokinin | KNO_3 | L-GLN | organic N | root growth | root system architecture

ABSTRACT

Nitrogen (N) availability is a key determinant of plant growth and development. Here, we investigate how different N sources shape *Arabidopsis thaliana* root system architecture, metabolism and hormone dynamics. L-glutamine (L-GLN) significantly enhances root biomass compared to nitrate (KNO_3) without compromising shoot growth. This effect emerges after 2 weeks and is independent of L-GLN's role as a carbon or ammonium source or of potential L-GLN-induced pH changes due to ammonium release, indicating a specific function of L-GLN as a N source and signaling molecule. A reverse genetic screen identified AMINO ACID PERMEASE 1 (AAP1)-mediated uptake and GLUTAMINE SYNTHETASE (GS)-dependent assimilation as essential for L-GLN-induced root biomass. In contrast, the N-sensing regulators NITRATE TRANSPORTER 1.1 (NRT1.1) and AMMONIUM TRANSPORTER (AMT) family members contribute to the differential root responses between KNO_3 and L-GLN. Metabolic profiling revealed distinct amino acid signatures under these N sources, irrespective of genotype. Hormonal analyses showed that L-GLN modulates auxin homeostasis, with auxin supplementation restoring primary root growth and lateral root symmetry under L-GLN conditions. L-GLN also reconfigures cytokinin balance by elevating cZ while reducing tZ, collectively shaping root system architecture through hormone-dependent regulation. Together, these findings establish L-GLN as an integrator of N metabolism and hormone signaling in root development, highlighting its signaling capacity beyond nutrient supply and offering new perspectives for improving N use efficiency.

1 | Introduction

N (Nitrogen) availability is essential for plant growth and development, and with growing concerns over agricultural sustainability, it is crucial to understand how different N sources affect plants. While inorganic N has been extensively studied, organic N sources have received less attention, despite their high abundance in soils, where organic N in the form of free amino acids typically occurs in the micromolar range and can represent a predominant N source in certain ecosystems (Inselsbacher and Näsholm 2012; Lipson and Näsholm 2001; Jämtgård et al. 2010). Plants can absorb various organic N forms, such as amino acids and proteins (Soldal and Nissen 1978; Chen and Bush 1995; Paungfoo-Lonhienne et al. 2008; Näsholm et al. 2009; Ganeteg et al. 2017), with AMINO ACID PERMEASES (AAPs) and LYSINE/HISTIDINE TRANSPORTERS (LHTs) facilitating their transport (Hirner et al. 2006). Organic N has been shown to promote growth, suggesting its role in specific signaling pathways (Walch-Liu et al. 2006; Näsholm et al. 2009; Cambui et al. 2011). In Arabidopsis, mutations or overexpression of LHT1 altered growth (Svennerstam et al. 2007), and GLUTAMATE RECEPTOR-LIKE (GLR) proteins, such as GLR3.2 and GLR3.6,

significantly affect root architecture (Singh et al. 2016). However, despite these findings, the mechanisms by which organic N influences plant development remain poorly understood.

L-glutamine (L-GLN) is a key amino acid with an active nutritional role across species. In plant tissue culture, L-GLN is commonly supplied at millimolar concentrations to promote rooting and shoot proliferation (Pedrotti et al. 1994; Pawar et al. 2015; El-Dawayati et al. 2018). L-GLN has been shown to increase biomass in Arabidopsis (Forsum et al. 2008) and rice (Kan et al. 2015) as well as enhance soluble protein and free amino acid content in hybrid maize (Hassan et al. 2020) when applied both as the sole N source (Forsum et al. 2008; Kan et al. 2015) and as a supplement to inorganic N (Hassan et al. 2020). However, as the exclusive N source, L-GLN has also been associated with reduced growth in wheat (Gioseffi et al. 2012) and inhibited root elongation in rice, Arabidopsis, and *Prunus cerasus* (Kan et al. 2015; Walch-Liu et al. 2006; Sarropoulou et al. 2012). These findings suggest that its positive impact on plant growth can be species- and/or organ-dependent and that additional research is required to understand the optimal conditions for its use.

Inorganic N, ammonium and particularly nitrate (NO_3^-) regulate lateral root (LR) development in a concentration-dependent manner, involving both local and systemic signals (Sun et al. 2017; Ohkubo et al. 2017). The 'dual pathway' model suggests that NO_3^- stimulates LR development through ion sensing at the plasma membrane, while its systemic inhibitory effect is associated with N status (Wang et al. 2012). NO_3^- affects various root processes, with NITRATE TRANSPORTER 1.1 (NRT1.1) acting as a key sensor (Riveras et al. 2015; Krouk 2017). AMMONIUM TRANSPORTERS (AMTs) regulate root branching (Loqué and von Wirén 2004; Lima et al. 2010), when pH-dependent auxin mobility plays a critical role in this response to ammonium (Meier et al. 2020). L-GLN regulates AMT1 expression, thereby controlling ammonium uptake in the plant. Subsequently, the GS/GOGAT cycle facilitates the assimilation of inorganic N into organic forms, such as L-GLN and glutamate (Rawat et al. 1999; Miflin and Habash 2002; Coruzzi 2003).

Plants adjust the growth and development of specific root parts to form a root system architecture (RSA) for optimum nutrient and water uptake, ultimately influencing plant fitness (Van Norman et al. 2013). RSA arises from differential growth dynamics across root regions (López-Bucio et al. 2003). On a larger scale, RSA describes the organization of primary and LRs, playing a key role in soil anchorage and resource efficiency. On a finer scale, root hairs increase surface area, enhancing water and nutrient uptake (Zygalakis et al. 2011; Gilroy and Jones 2000). Adventitious roots may also form post-embryonically at the root–shoot junction, particularly in response to nutrient-rich upper soil layers (De Klerk 1999; Geiss et al. 2009). In dicot plants like *Arabidopsis thaliana*, the root exhibits a hierarchical tree structure, with a primary root generating LRs, which in turn produce higher-order LRs. Even this fundamental structure can lead to diverse architectures through variations in LR emergence frequency and differential root growth rates (Hodge et al. 2009; De Smet et al. 2006).

RSA is influenced by external factors such as soil nutrient availability and internal regulators like plant hormones (Lavenus et al. 2013; Laplaze et al. 2007; Bielach et al. 2012). These factors integrate N signals to modulate growth and development in response to environmental changes (Gray 2004; Zhao et al. 2018). N signaling regulates the biosynthesis, transport, and activity of phytohormones, enabling plants to adapt to fluctuating N availability (Kiba et al. 2011; Ristova et al. 2016). Conversely, phytohormones regulate N uptake, signaling, and metabolism (Sakakibara et al. 2006; Kudo et al. 2010; Nacry et al. 2013; Ruffel et al. 2011).

This study focuses on the description of distinct RSA responses to KNO_3 and L-GLN as inorganic and organic N sources, respectively, in *Arabidopsis thaliana*. Although KNO_3 is assimilated into L-GLN after uptake, plant growth responses to these N sources differ significantly, highlighting L-GLN's role not only as a nutrient but also as a regulator of plant development. Our findings provide a comprehensive overview of the differential effects of KNO_3 and L-GLN on RSA, metabolism, and hormone dynamics, suggesting novel molecular players involved in these responses. These insights have potential applications in both traditional agriculture and soilless systems like hydroponics and aquaponics. While L-GLN is unlikely to serve as a sole N source in natural conditions, its ability to enhance growth and optimize N utilization alongside conventional fertilizers offers promising opportunities to improve N use efficiency and sustainability, particularly in controlled-environment agriculture.

2 | Materials and Methods

2.1 | Plant Material and Culture Conditions

All *Arabidopsis thaliana* plants studied in this work were homozygous for the mutations indicated. Single mutants *chl1.10* (Muños et al. 2004), *aap1* (Perchlik et al. 2014), *lht1* (Svennerstam et al. 2008), *lht6* (Perchlik et al. 2014), *glr3.1, glr3.2, glr3.3 and glr3.6* (Mousavi et al. 2013), multiple mutants *qko (amt1;1 amt1;2,1;3,2;1)* (Yuan et al. 2007), *gln tko (gln1.1;1.2;1.3)* (Moison et al. 2018) and *glr3.1/3.5* (Kong et al. 2016). The transgenic reporter lines *TCSn*::GFP (Zürcher et al. 2013) and *DR5v2*::ntdTomato (Liao et al. 2015) were previously described. The Nottingham Arabidopsis Stock Centre provided seeds for the wild type accession Col-0 (N1092), a putative *Fd-gogat* (SALK_018671)—hereinafter referred to as *gogat*—and *aap6* (Hunt et al. 2010) mutant lines. *chl1.10* mutant is in the Wassilewskija (Ws) accession background, but as both Col-0 and Ws ecotypes displayed the same growth responses to L-GLN (Figure S1), only Col-0 plants were used as controls in the experiments.

The presence and position of all insertions were confirmed by PCR amplification using gene-specific primers, together with insertion-specific primers (Table S1). In all experiments, the seeds were surface-sterilized by 70% ethanol with 0.1% Tween-20 and rinsed by 2 × 1 ml of 96% ethanol before being sown under sterile conditions on Petri dishes containing different kinds of media as described below. Stratification occurred at 4°C for 2 days and then plates were transferred to light at 22°C ± 1°C where the seedlings grew vertically in long-day light conditions (22°C, 16 h:8 h, light:dark) for a specific period of time depending on the experiment under

cool white fluorescent light (maximum irradiance 150 µmol $m^{-2} s^{-1}$). Further details on the length of the treatments are given in the captions of the respective figures.

2.2 | Media Preparation and Seedlings Treatments

Various types of Half Murashige & Skoog (½ MS; Murashige and Skoog 1962) media were used to select the optimized growing conditions: Duchefa M0222 (including vitamins and glycine), Duchefa M0221 (without vitamins and glycine), and ½ MS N-free basal salt micronutrient media (Merck M0529). M0221 medium was added to the screening of optimal growing conditions because of the presence of glycine, one of the amino acids studied, in the M0222 medium.

M0222 and M0221 media are fully supplemented with inorganic N forms ($KNO_3 + NH_4NO_3$ in final concentration of 30 mM N). M0222 medium was used for the amino acid screen and selection of candidate compounds (Figure S2A,B). M0221 medium was used to test the effect of selected amino acids in the absence of other organic N substances (such as vitamins and glycine, present in M0222) in the medium (Figure S2C,D).

Merck M0529 N-free medium was used for experiments with KNO_3, NH_4Cl or amino acids as an exclusive N source (Figures 2–6 and S1, S4–S7). The addition of macronutrients was performed to obtain the final concentration of ½ MS: CaCl (166 mg L^{-1}), KH_2PO_4 (85 mg L^{-1}), and $MgSO_4 \times 7\ H_2O$ (184 mg L^{-1}).

All types of media were additionally complemented with sucrose (10 g L^{-1}) and 2-(N-morpholine)-ethane sulphonic acid (MES) (0.5 g L^{-1}), the pH of the media was adjusted to 5.6, and subsequently, plant agar was added at a concentration of 7 g L^{-1}. Once sterile, the media were supplemented with filter-sterilized amino acid, KNO_3, or NH_4Cl to attain defined final concentrations. In addition, KCl was always added to balance the level of potassium in amino acid-treated media. Further details on specific N concentrations are given in the captions of the respective figures. For treatments with indole acetic acid (IAA), M0529 media were prepared and supplemented with various N sources as described above. DMSO as mock or 500 nM IAA was added to the media before plating. Plants were then grown for 15 days for phenotype evaluation.

2.3 | Root Phenotyping

For macroscopic root phenotyping (schematic overview in Figure 1A,B), the plates with seedlings were scanned with Epson Perfection V600 Photo, while for microscopic root phenotyping, photos of sequential root segments were taken using the Leica Widefield Thunder system with HC PL FLUOTAR L 20×/0.40 CORR PH1 objective. Quantification of RSA characteristics as shown in Figure 1B was performed using ImageJ software (Schindelin et al. 2015).

The phenotypic traits evaluated in this study:

Primary root length [cm]: Distance from the root tip to the root-hypocotyl junction.

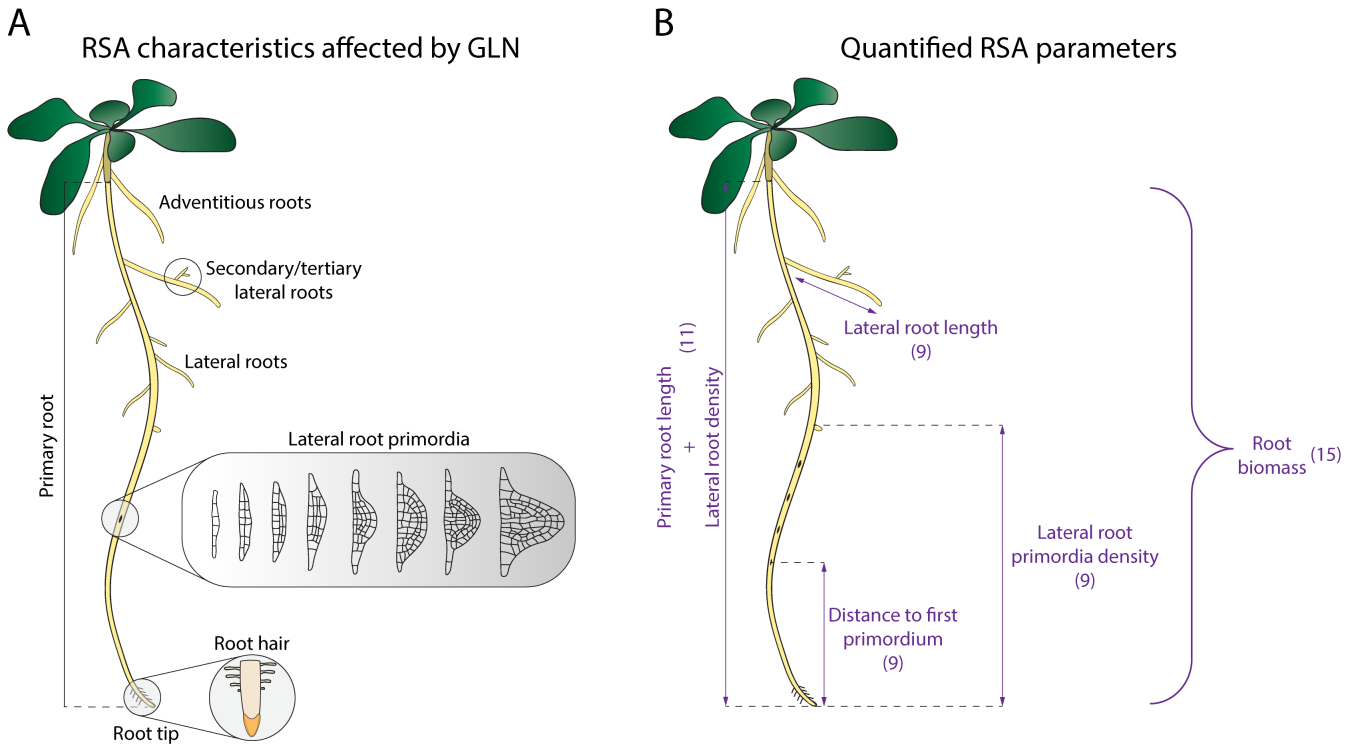

FIGURE 1 | General scheme of Arabidopsis root system architecture (RSA) evaluated in this study. (A) RSA characteristics contributing to the structural organization of RSA that are affected by L-GLN. (B) Quantitatively assessed RSA parameters in this study: Primary and LR length [cm]; distance from the primary root tip to the first primordium [mm]; LR density (number of LRs related to length of the primary root, #.cm^{-1}); LR primordia density (number of LRs related to the distance between the primary root tip and the first emerged LR, #.mm^{-1}); and root biomass (fresh weight of the root system, mg). Numbers in brackets indicate the age of the plants (in days) at the time of parameter evaluation.

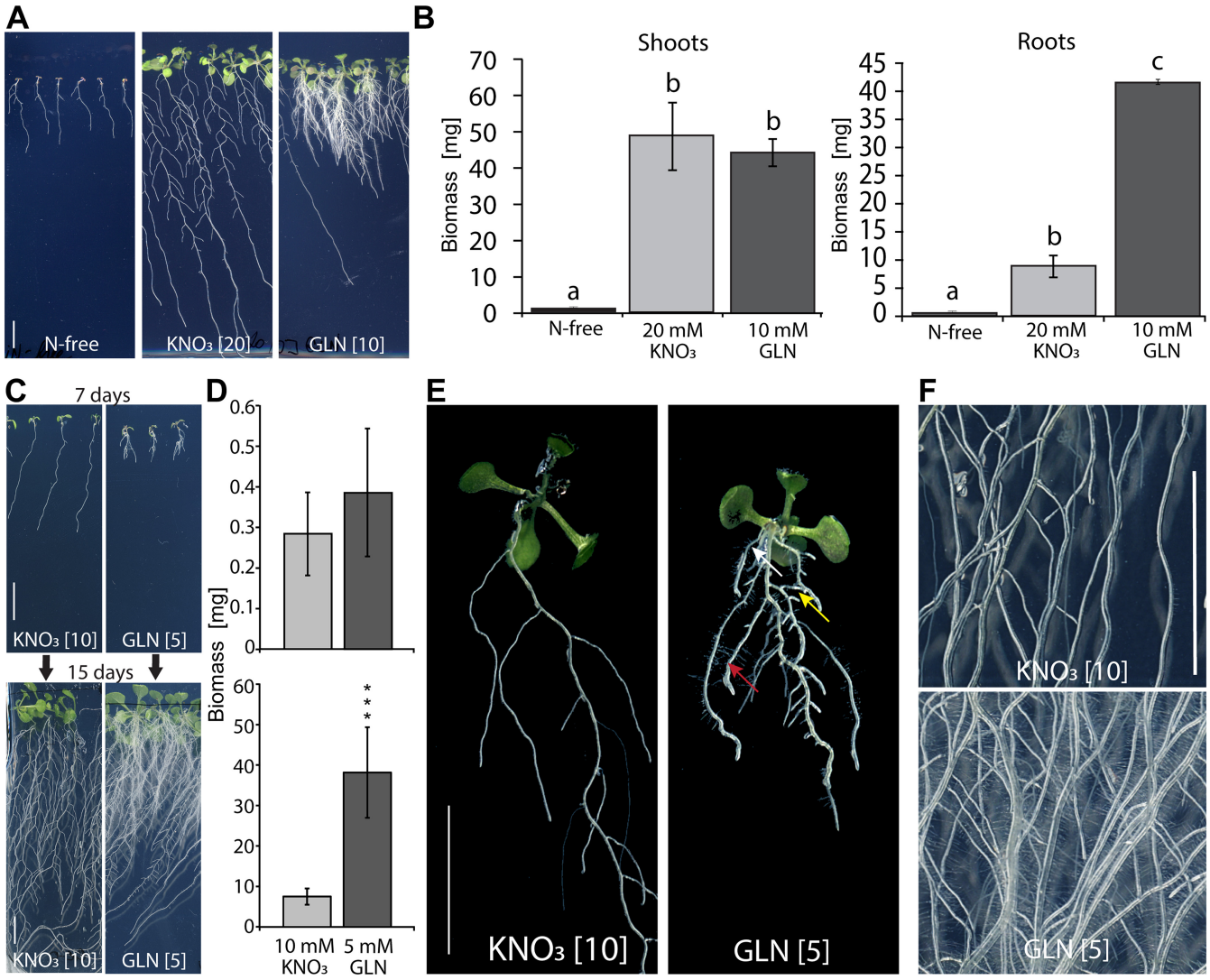

FIGURE 2 | L-GLN promotes root biomass and the growth of different RSA characteristics. (A, B) Representative phenotypes (A) and shoot and root biomass (fresh weight) (B) of Arabidopsis Col-0 plants grown in the absence of N or in the presence of 20 mM KNO_3 or 10 mM L-GLN for 15 days. (C) Representative phenotypes and (D) root biomass (fresh weight) of wild type plants grown in the presence of 10 mM KNO_3 or 5 mM L-GLN for 7 (upper panel) or 15 days (lower panel). (E) Closer look on the basal part of wild type seedlings grown in 10 mM KNO_3 or 5 mM L-GLN for 10 days, showing the distinct RSA. White arrow indicates adventitious roots, yellow arrow indicates secondary LRs, red arrow indicates root hairs. (F) Detailed picture of root hairs of wild type plants grown as described in (E) for 15 days. (A, C, E, F) Scale bar represents 1 cm, numbers in brackets are concentrations in mM. (B, D) Values are means ± SD; $n = 2$, each replicate represents a pool of 5 plants (B) and $n = 6$–10 individual plants (D). Statistical analyses were performed using the one-way ANOVA followed by Tukey's multiple comparisons test (B) and Student's *t*-test to compare individual treatments (D). Different letters indicate significant differences at $p < 0.05$ (B), *p*-values: ***$p < 0.001$ (D).

LR length [cm]: Distance from the LR tip to its base at the site of emergence from the primary root.

Total LR length [cm]: Sum of the lengths of all LRs per plant.

LR number [#]: Total number of LRs per plant.

LR density [#.cm^{-1}]: Number of LRs per unit length of the primary root.

LR primordia number [#]: total amount of LR primordia within the zone between the primary root tip and the first emerged LR.

LR primordia density [#.cm^{-1}]: Number of LR primordia per unit distance between the primary root tip and the first emerged LR.

Shoot and Root biomass [mg]: Fresh weight of the entire rosette/root system, respectively.

Because the different phenotypic traits mentioned above emerge at distinct developmental stages, plants were evaluated at different ages selected according to the timing of trait appearance and the practical requirements of the chosen evaluation method.

Given the pleiotropic effects of L-GLN on root development (Figure 1), we quantitatively assessed its impact on RSA

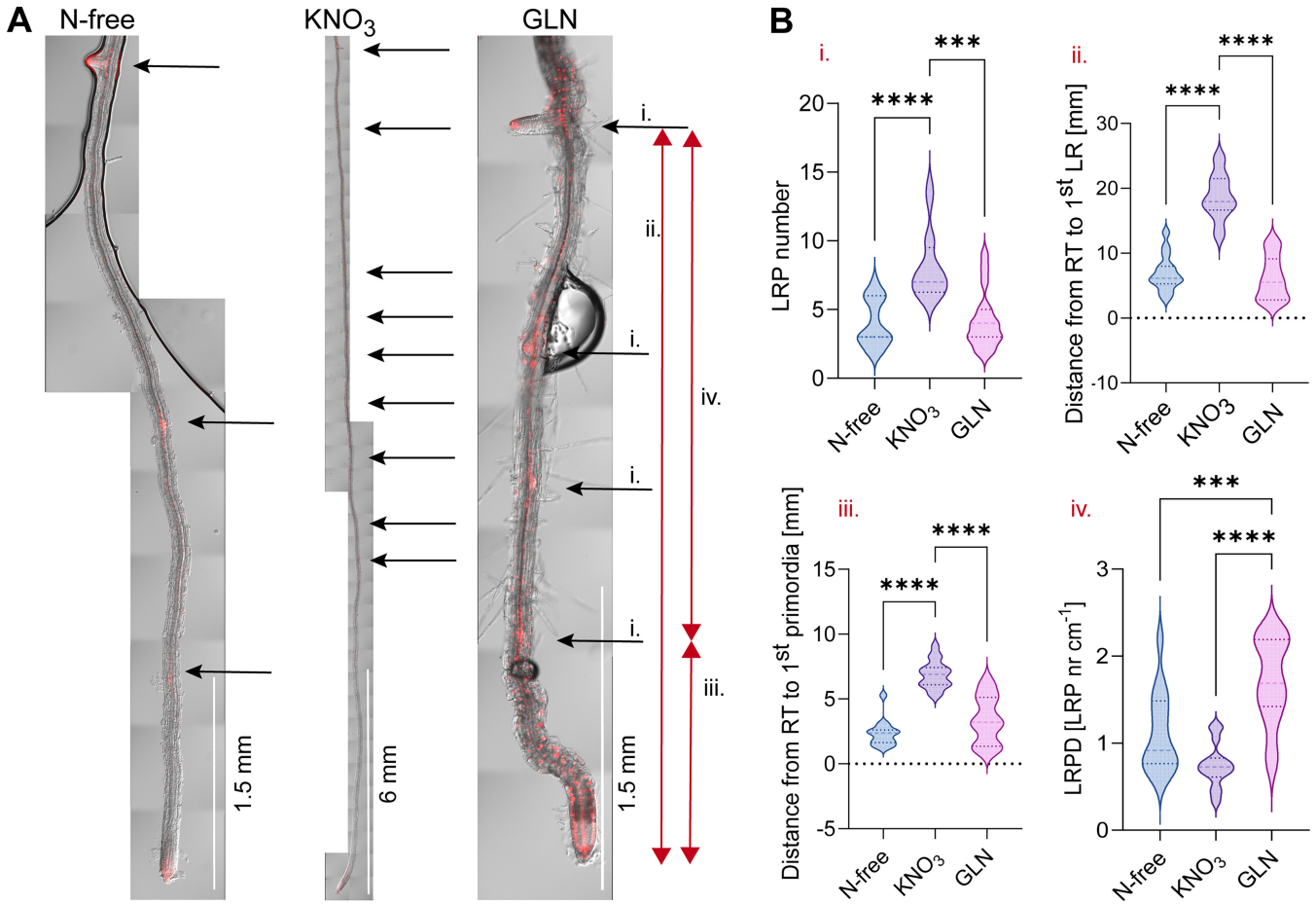

FIGURE 3 | LR patterning differs between L-GLN and KNO_3. (A, B) Microscopic pictures (A) and RSA parameters quantification (B) of Arabidopsis seedlings, expressing *DR5v2*::NtdTomato auxin reporter to visualize LR primordia, grown in the absence of N and in the presence of 10 mM KNO_3 or 5 mM L-GLN for 9 days. Arrows and lowercase roman numerals indicate individual parameters calculated in (B): Black arrows (i), red arrows (ii-iv). LR-LR, LRP-LR primordia, RT-root tip, LRPD-LR primordia density. (B) Violin plots display the distribution of the values, dotted lines in violin plots indicate first and third quartiles, centre line is median; $n = 16$ from four independent replicates. Statistical analyses were performed by ordinary one-way ANOVA followed by Tukey's test for normally distributed datasets (B-ii, iv), Kruskal-Wallis test for non-normally distributed datasets (B-i, iii) to compare individual N conditions; *p*-values: $^*p < 0.05$, $^{**}p < 0.01$, $^{***}p < 0.001$, $^{****}p < 0.0001$.

parameters in the Col-0 and Ws accessions by growing the seedlings under control conditions (10 mM KNO_3) for 5 days and then transferred to media containing either 10 mM KNO_3 or 5 mM L-GLN. The position of the primary root tip at the time of transfer was marked, and plants were cultivated for an additional 7 days. After this period, primary root length, LR number, and LR density below the transfer line (i.e., the portion of the root formed under the new conditions) were quantified.

2.4 | Fluorescent Microscopy

GFP expression patterns in 9-day-old *TCSn*::GFP, pCYCB1;1::GFP, and *DR5v2*::ntdTomato seedlings were recorded using Leica Widefield Thunder DMi8 (see above). GFP lines were imaged using BP 457-492 excitation and BP 508-551 emission filters; ntdTomato signal was visualized using BP 542-576 and BP 595-664 filters for excitation and emission, respectively. Fluorescent and TL-DIC microscopy pictures were taken by Leica DFC9000 GT camera. For display (not quantitative) purposes only, fluorescent pictures were processed by Leica Thunder Imager software to eliminate the out-of-focus blur.

2.5 | Image Processing and Statistical Analysis

All adjustments to the acquired scanned and fluorescent images were made using the ImageJ v.1.51w software (Schindelin et al. 2015). Fluorescent images were modified applying the same settings for each experimental dataset. The same applies for the scanned pictures except Figure 5, where different brightness and contrast were used to achieve comparable pictures from different plates for display (not quantitative) reasons only. The fluorescence intensity was quantified using the ImageJ v.1.51f software (Schindelin et al. 2015). Statistical analyses were conducted using two-sided independent Student's *t*-tests using Microsoft Excel or different ANOVA tests based on data distribution using GraphPad Prism 10.2.1 software. Further details of the statistics are given in the captions of the respective figures. The drawings were created using Adobe Illustrator.

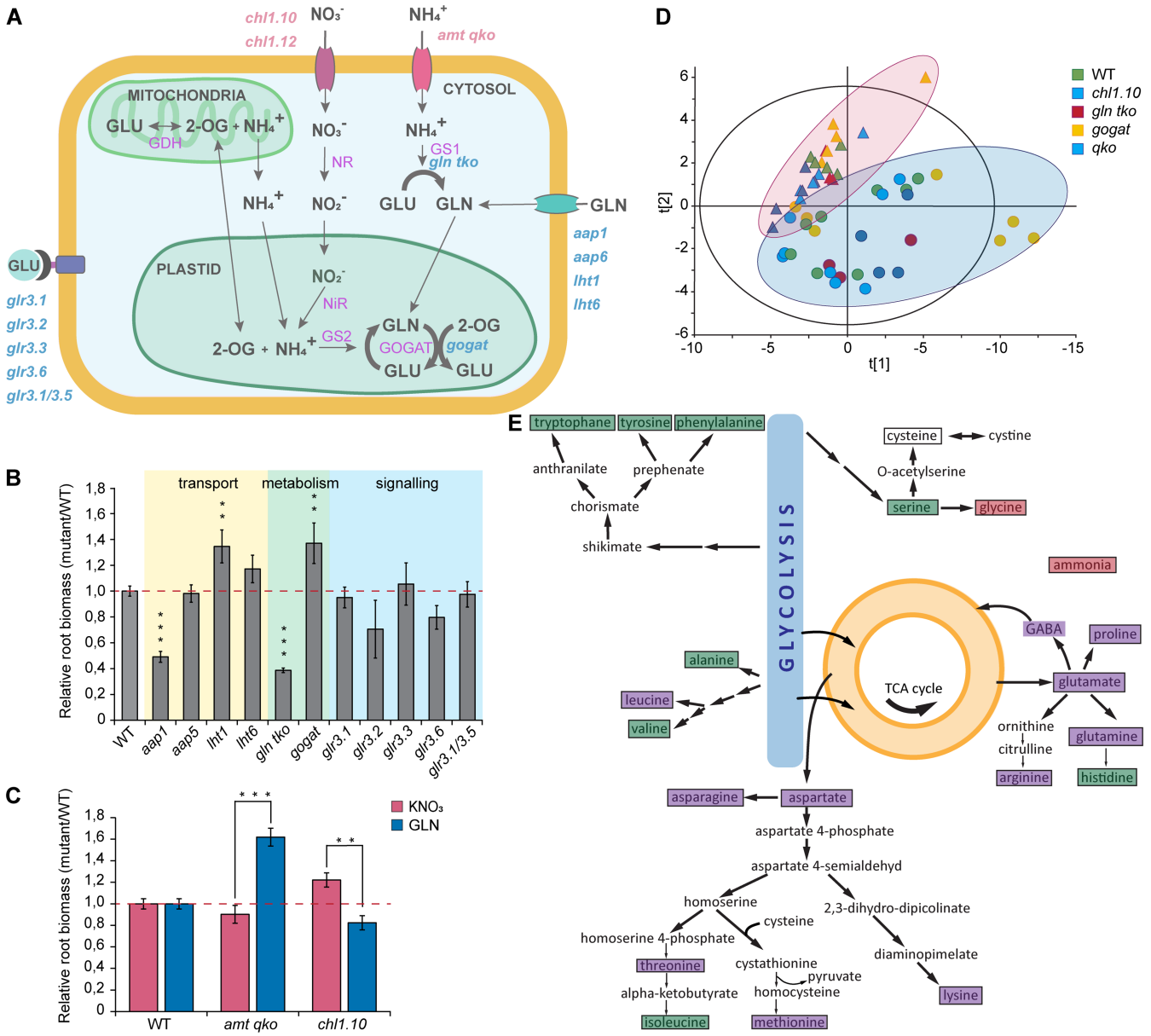

FIGURE 4 | Molecular players and key amino acids in L-GLN-dependent root outgrowth. (A) Simplified schematic of inorganic (magenta) and organic (blue) N transport, metabolism, and signaling sites investigated. (B) Root biomass of wild type and N-related mutants after 15 days in 5 mM L-GLN (B) or 10 mM KNO_3 /5 mM L-GLN (C). For complete dataset and statistical analysis of all mutants grown in both N conditions and more details on biomass evaluation, see Table S3. (B, C) Values are means ± SE (wild type: $N = 26–36$; mutants: $N = 3–9$ from 2 to 3 biological replicates). Statistical analyses: Student's *t*-test to compare mutants with wild type plants (B) or to compare KNO_3 and L-GLN treatments (C); *p*-values: $^{**}p < 0.01$, $^{***}p < 0.001$. (D) PCA (R2X(cum) 0.83, Q2 0.79) of samples from (B, C) showing distinct separation between KNO_3 (red) and L-GLN (blue) based on individual amino acid composition. PCA performed in SIMCA (v. 17.0.2.34594). Triangle and circle shapes represent KNO_3 and L-GLN treatments, respectively. Complete quantification and statistics of all amino acids quantified in all tested mutants are given in Dataset1. (E) Schematic overview of the main biosynthetic routes for amino acids (arrows indicate biosynthesis but all reactions are reversible). The color codes for different amino acids were based on a labeling experiment where amino acids were extracted from the roots of wild type seedlings grown in the presence of $^{13}C_5{}^{15}N_2$-L-GLN for 15 days. Based on their isotopic patterns, purple-colored compounds are proposed to be formed by direct conversion from L-GLN, green-colored compounds to be the receivers of one isotopically labelled atom from L-GLN in a stepwise pattern and red-colored compounds were detected as non-labelled. 2-OG, 2-oxoglutarate; aap, amino acid permease; amt, ammonium transporter; chl1, chlorina 1 (also known as nitrate transporter 1 (NRT1.1)); GABA, gamma-aminobutyric acid; GDH, glutamate dehydrogenase; GLN, glutamine; gln, GS mutant; glr, glutamate receptor; GLU, glutamate; GOGAT, glutamate synthase; GS, gln synthetase; lht, lysine histidine transporter; NiR, nitrite reductase; NR, nitrate reductase; TCA, tricarboxylic acid cycle.

2.6 | Feeding Experiments With Labelled GLN

Col-0 WT plants were grown in 6-well plates containing 5 mL of liquid N-free media (Merck, M0529—see above) supplemented with 10 mM KNO_3 or 5 mM $^{13}C_5{}^{15}N_2$ L-GLN (Merck) + 10 mM KCl for 15 days (light intensity 150 µmol·m^{-2}·s^{-1}, shaking conditions 95 RPM). After that, plant root samples were harvested from the media and directly deep-frozen in liquid N for the

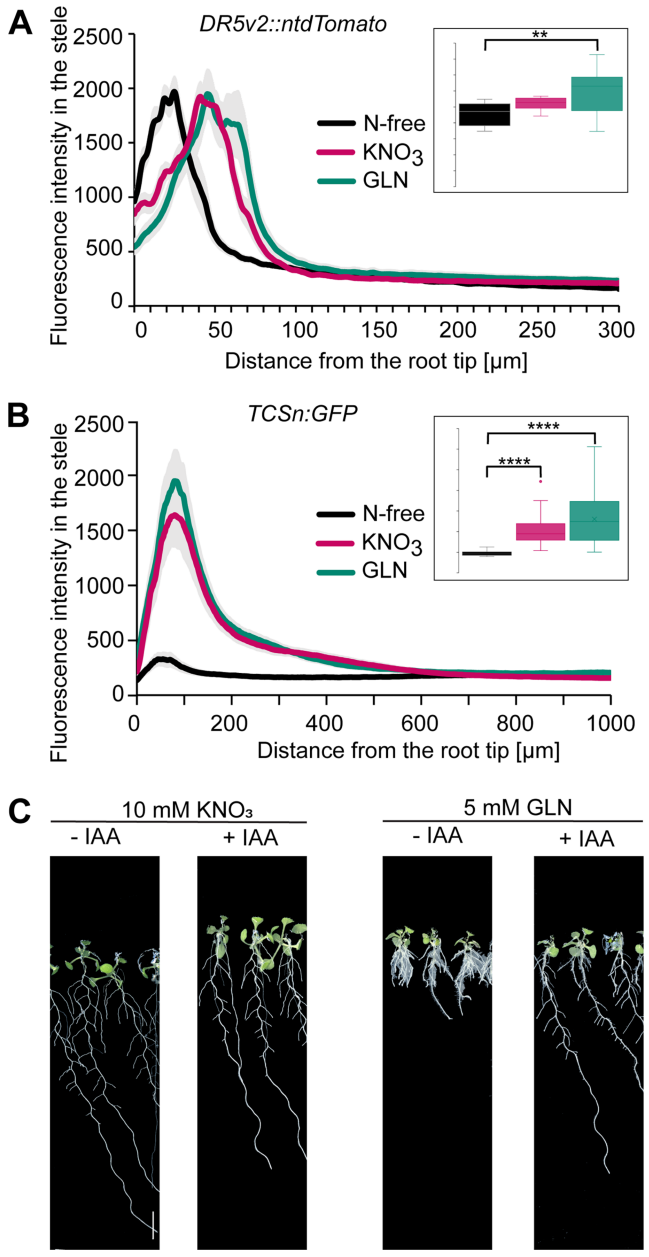

FIGURE 5 | Interplay of N and plant hormones in root responses. (A, B) Fluorescence intensity quantification in the primary root stele of *DR5v2*::NtdTomato (A) and *TCSn*::GFP (B) seedlings after 9 days in N-free, 10 mM KNO_3, or 5 mM L-GLN conditions. Data shows intensity as a function of distance from the root tip; inserts display mean intensity. Statistical analysis: One-way ANOVA with Tukey's test; $n = 14$ (A) from three replicates, $n = 15$–20 (B) from four replicates; p-values: $^{**}p < 0.01$; $^{****}p < 0.0001$. (C) Representative wild type *Arabidopsis* phenotypes after 15 days on 10 mM KNO_3 or 5 mM L-GLN, with or without 500 nM IAA. Scale bar: 1 cm.

liquid chromatography-mass spectrometry (LC–MS) analysis. In addition, 100 µL of media samples incubated in the presence or absence of plants were collected on day 0 and day 15 to evaluate GLN stability and uptake.

2.7 | Amino Acid Quantification—Derivatization

For amino acid quantification, 10 mg (FW) of root samples was extracted with 500 µL 80:20 (v/v) methanol:water solution containing norvaline as an extraction internal standard at 2.5 pmol/µl. The sample was shaken with a tungsten bead in a mixer mill (MM 400, Retsch) at 30 Hz for 3 min; the bead was removed, the sample was centrifuged at +4°C, 14000 rpm (18,620 × g) for 10 min, and the supernatant was collected. 10 µL of the supernatant was transferred to a microvial, evaporated to dryness, and stored at −80°C until analysis. A small aliquot of the remaining supernatants was pooled and used to create quality control (QC) samples. Blank samples, that is, samples without starting material, were prepared the same way as the plant samples.

Before analysis, the samples were derivatized by AccQ-Tag (Waters) according to the manufacturer's instructions. Briefly, the dried samples were dissolved in 20 µL 20 mM HCl, 60 µL of AccQ•Tag Ultra Borate buffer, including isotopically labelled internal standards (see Table S2 and Supporting Information), and finally 20 µL of the freshly prepared AccQ•Tag derivatization solution was added, and the sample was immediately vortexed for 30 s. The final concentration of the isotopically labelled internal standards was 0.5 pmol/µL. Samples were kept at room temperature for 30 min, followed by 10 min at 55°C. Calibration curves were prepared in a similar manner to the plant samples.

2.8 | Amino Acids Quantification by LC-ESI-MSMS

Derivatized samples were analyzed using a 1290 Infinity system from Agilent Technologies, consisting of G4220A binary pump, G1316C thermostated column compartment, and G4226A autosampler with G1330B autosampler thermostat coupled to an Agilent 6490 triple quadrupole mass spectrometer equipped with a jet stream electrospray source operating in positive ion mode.

Separation was achieved by injecting 1 µL of each sample onto a BEH C_{18} 2.1 × 100 mm, 1.7 µm column (Waters) held at 50°C in a column oven. The gradient eluents used were H_2O 0.1% formic acid (A) and acetonitrile 0.1% formic acid (B) with a flow rate of 500 µL/min. The initial conditions consisted of 0% B, and the following gradient was used with linear increments: 0.54–3.50 min (0.1%–9.1% B), 3.50–7.0 (9.1%–17.0% B), 7.0–8.0 (17.0%–19.70% B), 8.0–8.5 (19.7% B), 8.5–9.0 (19.7%–21.2% B), 9.0–10.0 (21.2%–59.6% B), 10.0–11.0 (59.6%–95.0% B), 11.0–11.5 (95.0% B), 11.5–15.0 (0% B). From 13.0 to 14.8 min, the flow rate was set at 800 µL/min for a faster equilibration of the column.

The MS parameters were optimized for each compound as described in Supporting Information. MRM transitions for the derivatized amino acids were optimized using MassHunter MS Optimizer software (Agilent Technologies Inc.). The fragmentor voltage was set at 380 V, the cell accelerator voltage at 7 V and the collision energies from 14 to 45 V; N was used as collision gas. Jet-stream gas temperature was 290°C with a gas flow of 11 L/min, sheath gas temperature 325°C, sheath gas flow of 12 L/min. The nebulizer pressure was set to 20 psi and the capillary voltage was set at 4 kV. The QqQ was run in Dynamic MRM Mode with 2 min retention time windows and

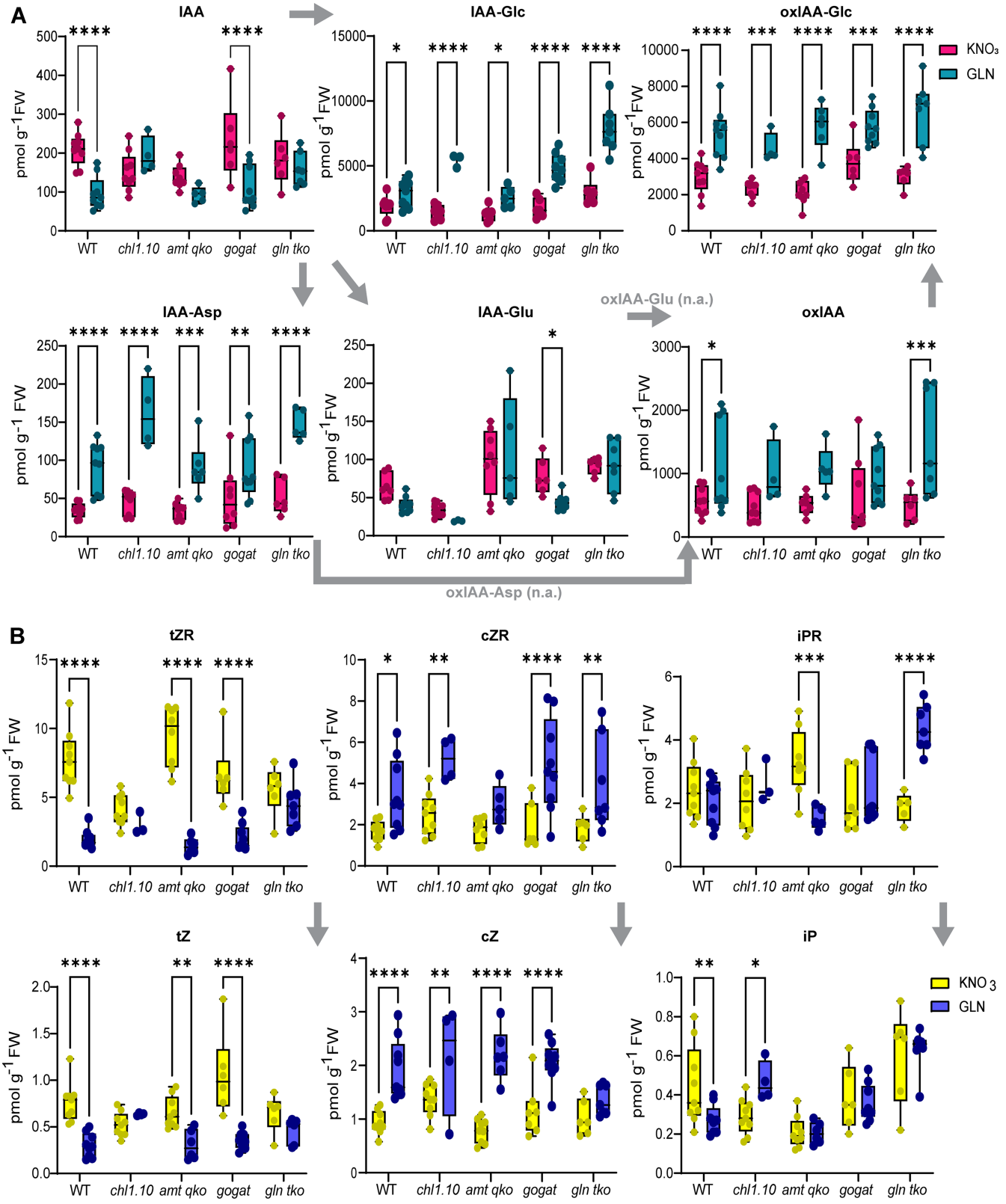

FIGURE 6 | Legend on next page.

500 ms cycle scans. For full information on MRM transitions, see Table S2.

The data was quantified using MassHunter Quantitation software B08.00 (Agilent Technologies Inc.) and the amount of each amino acid was calculated based on the calibration curves. Comparison of ammonium levels in KNO_3 and L-GLN-treated plants was performed by plotting the integrated peak area instead of calculated absolute concentrations because a suitable internal standard was not available.

FIGURE 6 | Effect of various N sources on hormonal dynamics. (A, B) LC–MS quantification of auxin, auxin metabolites (A), cytokinins and cytokinin precursors (B) in the roots of Arabidopsis wild type seedlings and different N-related mutant lines grown in the presence of 10 mM KNO_3 or 5 mM L-GLN for 15 days. Levels are expressed as pmol per g of root fresh weight (FW). Grey arrows represent metabolic pathways. Boxes indicate first and third quartiles, whiskers represent variability outside the quartiles, dots are individual values and the centre line is the median, $n = 4–9$ from three independent replicates. Statistical analyses were performed by two-way ANOVA followed by Tukey's test to compare the hormonal levels between the genotypes and between N conditions; p-values: *$p < 0.05$, **$p < 0.01$, ***$p < 0.001$, ****$p < 0.0001$. cZR, cis-zeatin; cZR, cis-zeatin riboside; IAA, indole-3-acetic acid; IAA-Asp, IAA-aspartate; IAA-Glc, IAA-glucosyl ester; IAA-Glu, IAA-glutamate; iP, isopentenyl adenine; iPR, isopentenyl adenine riboside; n.a., not analysed; oxIAA, 2-oxoindole-3-acetic acid; oxIAA-Glc, oxIAA-glucosyl ester; tZR, trans-zeatin; tZR, trans-zeatin riboside.

2.9 | Tracer Experiment and LC-ESI-QTOFMS Analysis

For tracer experiments, 10 mg (FW) plant material was extracted with 1000 µL extraction solution 80:20 (v/v) Methanol: water without internal standards, following the same extraction protocol as the amino acid quantification. For liquid media, 100 µL of media was extracted with 900 µL of 90:10 (v/v) Methanol. For analysis, 20 µL of the corresponding supernatant was transferred to microvials, evaporated to dryness, and derivatized following the same protocol as for the amino acid quantification.

The chromatographic separation was performed on an Agilent 1290 Infinity UHPLC system (Agilent Technologies) using the same chromatographic setup as for amino acid quantification. The compounds were detected with an Agilent 6546 Q-TOF mass spectrometer equipped with a dual jet stream electrospray ion source operating in positive ion mode. Purine (4 µM) and HP-0921 [Hexakis(1H, 1H, 3H-tetrafluoropropoxy)phosphazine] (1 µM) were infused directly into the MS at a flow rate of 0.05 mL $m\,in^{-1}$ for internal mass calibration and accurate mass measurements; the monitored ions were purine m/z 121.05 and HP-0921 m/z 922.0098. The gas temperature was set to 150°C, the drying gas flow to 8 L min^{-1}, and the nebulizer pressure 35 psig. The sheath gas temp was set to 350°C and the sheath gas flow to 11 L min^{-1}. The capillary voltage was set to 4000 V in positive ion mode. The nozzle voltage was 300 V. The fragmentor voltage was 120 V, the skimmer 65 V, and the OCT 1 RF Vpp 750 V. The collision energy was set to 0 V. The m/z range was 70–1700, and data were collected in centroid mode with an acquisition rate of 4 scans s^{-1} (1977 transients/spectrum).

All data pre-processing was performed using the Agilent Masshunter Qual version B.07.00 (Agilent Technologies Inc.).

2.10 | Auxin and Cytokinin Measurements

The roots of wild type and mutant plants grown on 10 mM KNO_3 or 5 mM L-GLN media for 15 days were collected and directly frozen in liquid N until hormone purification and analysis.

For cytokinin (CK) analysis, 10 mg of root fresh weight per sample was homogenized and extracted in 0.5 mL of a modified Bieleski buffer consisting of 60% (v/v) MeOH, 10% (v/v) HCOOH, and 30% (v/v) H_2O. A mixture of stable isotope-labeled internal standards (0.25 pmol of CK bases, ribosides, N-glucosides, and 0.5 pmol of CK O-glucosides, nucleotides per sample) was added for further quantification. The purification of CKs was carried out using in-tip solid-phase micro-extraction based on the StageTips technology, as previously described by Svačinová et al. (2012). This involved the activation of combined multi-StageTips containing C18/SDB-RPSS/Cation-SR layers with sequential washes with 50 µL of acetone, methanol, water, 50% (v/v) nitric acid, and water employing centrifugation at 434 × g, 15 min, 4°C. After the application of the sample (500 µL, 678 × g, 30 min, 4°C), the microcolumns were washed with 50 µL of water and methanol (525 × g, 20 min, 4°C), followed by elution with 0.5 M NH_4OH in 60% (v/v) methanol (525 × g, 20 min, 4°C). The eluates were then evaporated and stored at −20°C. The quantitative analysis of the CK profile was performed using multiple reaction monitoring with an ultra-high performance liquid chromatography-electrospray tandem mass spectrometry (UHPLC–MS/MS) system. The separation was carried out on an Acquity UPLC i-Class System (Waters) with an Acquity UPLC BEH Shield RP18 column (150 × 2.1 mm, 1.7 µm; Waters), and the effluent was introduced into the electrospray ion source of a triple quadrupole mass spectrometer Xevo TQ-S MS (Waters).

Auxin analysis was performed as described in Pěnčík et al. (2018). Briefly, approx. 2.5 mg of roots were extracted in 50 mM phosphate buffer (pH 7.0) containing 0.1% sodium diethyldithiocarbamate and stable isotope-labeled internal standards. 200 µL of each extract was acidified to pH 2.7 using 1 M HCl and purified by in-tip micro solid-phase extraction (in-tip µSPE). After evaporation, samples were analyzed using HPLC system 1260 Infinity II (Agilent Technologies) equipped with Kinetex C18 (50 × 2.1 mm, 1.7 µm; Phenomenex Torrance). The LC system was linked to a 6495 Triple Quad mass spectrometer (Agilent Technologies).

CK and auxin concentrations were determined using MassLynx software (v4.2; Waters) and Mass Hunter software (version B.05.02; Agilent Technologies), respectively, using the stable isotope dilution method.

3 | Results

3.1 | L-Glutamine Promotes Root Biomass and Serves as a Sufficient N Source

L-GLN was selected as the optimal organic N source because its addition to KNO_3-containing media consistently enhanced lateral root (LR) length (Figure S2A), LR density (Figure S2B), and

increased both shoot and root biomass (Figure S2C,D) across various concentrations and growing conditions—presence/absence of sucrose (Figures S2B and S3) or vitamins + glycine (Figure S2A–D) in the media—outperforming most other amino acids. Since amino acids supply both N and carbon, we examined whether their carbon contribution influenced LR density. Plants were grown in amino acid-supplemented media with or without sucrose. While sucrose affected primary root length, it did not alter the increase in LR density observed with amino acid supplementation compared to KNO_3 alone (Figure S2B). It should be noted that while the effect of L-GLN on primary root length could be variable, the increased biomass and LR phenotypes, being the primary focus of this study, were reproducible in all cases.

To determine whether L-GLN alone provides a comparable N source, plants were grown in media that were either N-free (N-free) or supplemented with KNO_3 or L-GLN (Figure 2A,B). N concentrations were adjusted to ensure equal N availability based on molecular composition (KNO_3 vs. L-GLN: $C_5H_{10}N_2O_3$). Further observations revealed that the substantial increase in root biomass seen in plants grown in L-GLN was time-dependent (Figure 2C,D) and primarily attributed to a higher number of lateral and adventitious roots, increased LR orders, and enhanced root hair development (Figure 2E,F).

3.2 | L-Glutamine and KNO_3 Differentially Modulate Root System Architecture

To assess how L-GLN and KNO_3 influence RSA characteristics, we analyzed 9-day-old *Arabidopsis* seedlings expressing *DR5v2*:ntdTomato, a reporter for auxin signaling and LR primordia. Seedlings grown on KNO_3 exhibited a significantly higher number of LR primordia in the region between the root tip and the first emerged LR compared to those grown on L-GLN or N-free media (Figure 3A,B). However, this region was significantly shorter under L-GLN and N-free conditions, resulting in a higher density of LR primordia. The distance from the root cap to the first LR primordium was also significantly decreased in response to L-GLN treatment (Figure 3A,B).

As both ammonium and changes in ambient pH are known to influence RSA (Meier et al. 2020; Duan et al. 2023), we tested the hypothesis that the L-GLN–induced phenotypes might result from ammonium release and associated pH shifts. Low ammonium concentrations did not reproduce the effects of L-GLN, while high concentrations were toxic (Figures S4A,B and S5). Moreover, ammonium levels in L-GLN–treated plants were not higher than in KNO_3-treated plants (Figure S4C), indicating that ammonium release is not responsible for the observed phenotypes. Finally, the pH of the growth media remained stable across treatments (Figure S4D), excluding pH fluctuations as a contributing factor to the L-GLN–induced phenotypes.

Feeding experiment with labeled L-GLN showed that the compound was fully absorbed within 15 days, leaving no detectable residue in the media (Figure S4E,F). Notably, supplying additional L-GLN after this period further enhanced biomass (Figure S4G), consistent with its role as a positive root growth regulator. However, whether the observed effects reflect continuous external uptake or utilization of L-GLN internal pools accumulated during the first days of the treatment cannot be distinguished.

3.3 | Dissecting L-Glutamine's Mode of Action in Root Outgrowth: Insights From a Genetic Screen and Amino Acid Analysis

To investigate how L-GLN regulates root growth, we conducted a reverse genetic screen on mutants deficient in L-GLN assimilation (*gogat* and *gln tko*), transport (*aap1, aap5, lht1, lht6*), and signaling (*glr3.1, glr3.2, glr3.3, glr3.6, glr3.1/3.5*). A summary of these genes' functions is provided in Figure 4A. The screen revealed that mutants lacking *AAP1*-mediated transport or impaired in the conversion of glutamate to L-GLN via the *GLN SYNTHETASE (GS)* gene family exhibited significantly reduced biomass compared to wild type plants grown on L-GLN (Figure 4B, Table S3A,B). Interestingly, *lht1* and *gogat* mutants displayed increased root biomass relative to wild type plants under L-GLN treatment (Figure 4B). In contrast, *glr* mutants showed no significant differences in biomass (Figure 4B).

A secondary screen of inorganic N transport mutants (*amt qko* and *chl1.10*) was performed, investigating the differential response between L-GLN and KNO_3 for mutants relative to WT (similar fold-increase in biomass in a mutant and in WT considered as the same response), making the effect L-GLN-specific. The CHL1 and AMTs mutants were chosen because their function lies not only in transport but also as central components of N signaling cascades, whose activity can be modulated by organic N sources (Walch-Liu and Forde 2008; Ho et al. 2009; Mounier et al. 2013; Rawat et al. 1999; Kojima et al. 2023; Javelle et al. 2003) such as L-GLN. The results revealed that the relative mutant/WT root biomass was higher for *amt qko* mutants when grown on L-GLN compared to KNO_3, whereas *chl1.10* mutants exhibited the opposite trend, displaying reduced mutant/WT biomass ratio under L-GLN treatment (Figure 4C, Table S3).

To investigate whether the differences in mutant root responses to L-GLN are associated with changes in amino acid profiles, we conducted an amino acid analysis on mutants that showed significant biomass changes in the reverse genetics screen (Figure 4B,C), excluding L-GLN transporters. The PCA analysis revealed distinct metabolic profiles depending on N treatment with L-GLN-fed plants (Figure 4D) accumulating higher levels of L-GLN, alanine, GABA, citrulline, and glycine, whereas isoleucine and tyrosine were more abundant in KNO_3-fed plants (Figure S6A,B). However, the variation in amino acid profiles was insufficient to clearly separate mutants with distinct root phenotypes (Figure 4D), suggesting that the observed differences in root responses cannot be fully explained by differences in their amino acid profiles.

Long-term feeding experiments with labeled L-GLN demonstrated its incorporation into all detected amino acids, indicating two main metabolic routes of N assimilation (Figures 4E and S6). One group of amino acids (marked purple in Figures 4E and S7B) showed multiple isotopically labeled atoms, suggesting direct conversion from L-GLN. A second group (marked green in Figures 4E

and S7C) exhibited a stepwise incorporation pattern, indicating the transfer of a single labeled atom from L-GLN into these amino acids.

3.4 | L-Glutamine Effects on Root Growth Are Linked to Hormonal Dynamics

Since the distinct differences in root responses of WT and mutant plants could not be attributed to amino acid composition (Figure 4C), we examined whether the phytohormones auxins and cytokinins contribute to the L-GLN- and KNO_3-induced differential root growth responses. These hormones strongly interact at the primary root tip—where initial steps of LR formation take place—and thus strongly regulate RSA characteristics (Aloni et al. 2006).

Auxin (*DR5v2*::ntdTomato) and cytokinin (*TCSn*::GFP) reporter lines were used to visualize hormonal responses in the primary root meristem and pre-branch site formation zone. Fluorescence quantification showed no significant differences in auxin or cytokinin signaling between plants grown on L-GLN and KNO_3 (Figure 5A,B). However, supplementing auxin to L-GLN-containing media restored primary root growth and normalized LR symmetry (Figure 5C), suggesting that L-GLN affects auxin homeostasis.

To further explore hormonal regulation under different N conditions, auxin and cytokinin metabolite levels were quantified via mass spectrometry in wild type plants, as well as in the mutants previously investigated for their amino acid profiles (Figure 4D).

Wild type plants grown on L-GLN had lower levels of bioactive indole-3-acetic acid (IAA) compared to those on KNO_3, while most IAA conjugates, except IAA-Glu, were significantly enriched in L-GLN-treated plants (Figure 6A). Cytokinin quantification showed decreased trans-zeatin (tZ) and isopentenyl adenine (iP) levels in L-GLN-grown wild type plants, whereas cis-zeatin (cZ) levels were elevated compared to those grown in KNO_3 (Figure 6B). Additionally, in *gln tko* mutants, iP compounds exhibited differential abundance in response to KNO_3 and L-GLN compared to wild type plants. Despite this variation, overall hormone concentration patterns remained consistent across all mutants, suggesting that auxin and cytokinin regulation is more strongly influenced by the N source than by disruptions in N uptake and assimilation.

4 | Discussion

L-GLN, a key amino acid in plant N metabolism, not only serves as a N source but also plays a crucial role in modulating RSA. L-GLN effects on root growth are shown to be a complex response dependent on the concentration applied (Figures S2A,C, S3A,B, S5), the duration of application (Figure 2C,D) and the interaction with other N sources (when applied together with inorganic N; Figure S2). Our study highlights L-GLN's ability to significantly enhance root biomass independently of its role as a carbon source and proposes specific transport, metabolic and hormone-interacting pathways that are involved in L-GLN root responses.

4.1 | L-Glutamine as a N Source Enhances Root Biomass

Our results demonstrate that, in contrast to many amino acids that inhibit root growth, L-GLN consistently promoted root biomass at biologically relevant (μM) concentrations, even in the presence of abundant KNO_3 (Figures 2 and S1). These findings indicate a dual function of L-GLN as both a nutrient and a signaling molecule, a role not previously reported. This aligns with recent findings showing that L-GLN is associated with a distinct phenotype characterized by extensive root and root hair development that optimizes uptake of less mobile N forms (Tünnermann et al. 2025), improves amino acid use efficiency (Lardos et al. 2023), and arginine, asparagine, and histidine levels in both roots and shoots (Svietlova et al. 2024). Our results highlight the specificity of L-GLN, as its positive effects on root biomass were independent of pH changes or ammonium release (Figure S4). Although amino acids influence RSA in various ways (Figures 2 and S2; Ravelo-Ortega et al. 2021; Montiel and Dubrovsky 2024), it is unclear whether L-GLN's effects are unique or part of a broader response to organic N sources. More complex N sources, such as proteins, can also enhance root biomass (Paungfoo-Lonhienne et al. 2008; Lonhienne et al. 2014), but their effects may arise from protein-specific signaling or the release of amino acids like L-GLN during protein degradation. Notably, L-GLN's positive growth effects have been observed across various species, including *Arabidopsis* (Forsum et al. 2008; Lardos et al. 2023), rice (Kan et al. 2015), and symbiotic species such as poplar (Han et al. 2022).

Interestingly, L-GLN's root-promoting responses were observed even in the absence of an external carbon source, such as sucrose (Figures S2 and S3). While sucrose increased overall LR density, consistent with its roles as both a carbon source and a signaling molecule that positively influences RSA parameters (Takahashi et al. 2003; MacGregor et al. 2008; Zhang et al. 2020), the relative responses to amino acids were preserved, suggesting that amino acid and sugar-mediated pathways act in a partially independent and additive manner. Although GLN-derived carbon contributes to the positive effects of L-GLN (Tünnermann et al. 2025), our results indicate that it is not the main driver of L-GLN's stimulatory effects on root growth. This conclusion is further supported by the distinct effects of L-GLN and glutamate on root biomass relative to KNO_3 (Figure S2A; Lardos et al. 2023), despite their shared carbon backbone, suggesting L-GLN-specific impact on root development.

4.2 | Distinct Mechanisms of L-Glutamine and KNO_3 in Root Growth Regulation

When supplied in equimolar N amounts, L-GLN supported plant development comparably to KNO_3 and even outperforms it in root-specific biomass accumulation (Figure 2A,B). Notably, L-GLN's effects on root biomass became more pronounced over time, particularly after 15 days (Figure 2C,D), which is consistent with Lonhienne et al. (2014)'s conclusion that N sources influence the timing of LR initiation in Arabidopsis.

Detailed root morphology analysis revealed that L-GLN enhances RSA complexity by increasing LR density, adventitious

root number, higher-order branching, and root hair elongation (Figure 2E,F). Similar findings were observed in split-root experiments, where localized N sources favored L-GLN over KNO_3 (Tünnermann et al. 2025). Additionally, L-GLN-grown plants exhibited a shorter distance between the root cap and the first emerged LR, suggesting an accelerated LR initiation program (Figure 3). This aligns with studies demonstrating that organic N sources modulate LR initiation and emergence through mechanisms distinct from KNO_3-dependent signaling (Cambui et al. 2011; Han et al. 2022).

4.3 | L-Glutamine Uptake; L-Glutamine/L-Glutamate Metabolism and Signaling in L-GLutamine-Mediated Root Growth

Amino acid uptake is mediated by both low- and high-affinity transporters, depending on ambient N availability (Yao et al. 2020). Here, we show that AAP1 is critical for L-GLN–mediated root growth (Figure 4B), consistent with previous reports showing reduced L-GLN uptake in *aap1* mutants at high substrate concentrations (Lee et al. 2007). In contrast, *lht1* mutants, which are impaired in high-affinity L-GLN uptake at low concentrations (Hirner et al. 2006; Svennerstam et al. 2011), displayed enhanced root growth. At 5 mM L-GLN, transport can be efficiently mediated by lower- or medium-affinity transporters such as AAPs (Yao et al. 2020). Additionally, compensatory upregulation of other transporters like AAP5 in *lht1* (Svennerstam et al. 2011) may further facilitate uptake, explaining the increased biomass observed.

In *Arabidopsis thaliana*, GOGAT enzymes play a central role in N assimilation and amino acid biosynthesis, which has implications in various developmental processes. GLU1 is expressed at the highest levels in leaves, playing a major role in photorespiration, and complete loss of GLU1 is lethal (Coschigano et al. 1998). In contrast, GLU2 is preferentially accumulated in roots and GLU2 mutants are viable (Coschigano et al. 1998), enabling us to investigate their role in L-GLN responses. The phenotypes of the *gs tko* and *gogat* mutants highlight the complexity of L-GLN metabolism in roots. Surprisingly, both mutants showed improved growth upon L-GLN feeding compared to nitrate, despite their impaired capacities in L-GLN synthesis or utilization (Table S3A). These results suggest that the observed responses are not due to N starvation, consistent with Svietlova et al. (2024) who found no induction of the N deficiency markers NRT2.4 or NRT2.5. Instead, our data suggest that L-GLN triggers regulatory mechanisms beyond its role as a N source, pointing to a more complex control of root development by amino acid signaling. Notably, *lht1* and *gogat* mutants exhibited increased biomass specifically under L-GLN conditions, suggesting roles in modulating L-GLN-specific responses. One possibility is that LHT1 and GOGAT regulate the internal concentration and metabolic fate of L-GLN, thereby influencing signaling or feedback mechanisms linked to growth. Impaired GOGAT activity may disrupt the assimilation of L-GLN-derived N into downstream metabolites, altering N sensing or metabolic programming in ways that favor biomass accumulation. This supports our hypothesis that L-GLN functions not only as a nutrient source but also as a signaling molecule shaping root architecture.

Interestingly, the impairment of GLR-mediated signaling did not affect root biomass under L-GLN conditions (Figure 4B). Although GLR3.2 and 3.4 are involved in LR initiation (Vincill et al. 2013), microscopic changes in LR primordia density may have been missed in the total biomass assessment.

4.4 | Molecular Components in L-Glutamine- and KNO_3-Grown Plants

A secondary screen of *chl1.10* and *amt qko* mutants was performed to investigate how CHL1 and AMTs function as signaling components in N-dependent root development, independently of nitrate or ammonium availability. CHL1 acts as a nitrate sensor influencing RSA in response to both nitrate and glutamate (Walch-Liu and Forde 2008; Ho et al. 2009; Mounier et al. 2013), while AMT expression and activity are tightly regulated by L-GLN and downstream N assimilation products (Rawat et al. 1999; Kojima et al. 2023; Javelle et al. 2003). Studying these mutants in the absence of nitrate and ammonium allowed us to specifically probe L-GLN-dependent signaling in root development.

Our results indicate that L-GLN and KNO_3 activate distinct developmental pathways controlling root growth. Both *amt qko* and *chl1.10* showed significant differences in root biomass when grown on L-GLN versus KNO_3 (Figure 4B, Table S3), highlighting their roles in mediating responses to organic N.

In *amt qko* mutants, total dry weight was significantly reduced compared to wild type when ammonium was supplied, but remained unchanged under KNO_3 (Lima et al. 2010). Interestingly, when grown on L-GLN, *amt qko* exhibited increased root biomass relative to wild type (Figure 4C, Table S3), consistent with the idea that AMT-dependent signaling can negatively regulate root growth in the presence of L-GLN. This is supported by evidence that *AtAMT1* expression and high-affinity ammonium influx are suppressed by L-GLN accumulation (Rawat et al. 1999). Similarly, induction of ammonium assimilation genes, such as *GLN1;2* and *GLT1*, is mediated by L-GLN rather than ammonium itself (Kojima et al. 2023). Thus, L-GLN acts as a feedback signal modulating AMT expression and ammonium metabolism. Moreover, AMTs repress LR development in the presence of ammonium (Lima et al. 2010), suggesting that they act as key regulators linking N signaling to root developmental programs.

Several hypotheses could explain the enhanced growth of *amt qko* on L-GLN, including compensatory upregulation of other amino acid transporters, altered root architecture facilitating L-GLN uptake, or more favorable metabolic partitioning of supplied L-GLN, such as more efficient assimilation or lower energetic cost.

The *chl1.10* mutant, on the other hand, exhibited reduced root biomass on L-GLN compared to nitrate (Figure 4C, Table S3), consistent with previous findings that CHL1/NRT1.1 influences root development under both nitrate and organic N regimes (Walch-Liu and Forde 2008; Ho et al. 2009; Mounier et al. 2013). For example, *chl1.10* mutants exhibit reduced LR stimulation under localized high nitrate (Remans et al. 2006) and increased LR density under low nitrate or low L-GLN (Krouk et al. 2010), suggesting that CHL1 integrates multiple N

cues. Interestingly, the observed mutant phenotypes were not directly linked to absolute L-GLN levels as both *amt tko* and *chl1.10*, which showed distinct L-GLN responses (Figure 4C), had similar L-GLN concentrations (Figure S6C). Notably, *amt tko* accumulated the least L-GLN, yet exhibited the highest biomass increase, indicating that differential signaling rather than uptake efficiency underlies the observed responses.

Data from split-root experiments (Tünnermann et al. 2025) showed that local L-GLN supply strongly alters RSA—enhancing root mass and root hair length—even when nitrate is available elsewhere. This supports the hypothesis that CHL1-dependent signaling integrates local and systemic N cues, and that L-GLN itself can act as a signaling molecule regulating root development.

Overall, our results highlight that CHL1 and AMTs function not only as transporters but also as regulatory nodes within the N signaling network. Their activity determines how plants interpret the balance of N forms, underscoring L-GLN's role in modulating RSA mediated through regulators traditionally associated with inorganic N.

4.5 | Metabolic and Hormonal Regulation in L-Glutamine- and KNO_3-Grown Plants

Isotopic labeling revealed distinct metabolic routes for L-GLN assimilation, with some amino acids directly converted from L-GLN, while others show an incorporation pattern that suggests one (or in some cases two) isotopically labelled atoms are incorporated in a stepwise pattern (Figures 4E and S7B,C). Our results demonstrate that labeled atoms from L-GLN were incorporated into almost all identified amino acids through these two distinct metabolic routes (Figure 4E), underscoring L-GLN's central role in plant N metabolism.

Metabolite profiling indicated that N source, rather than genotype, drives variation in amino acid composition. L-GLN-fed plants accumulated L-GLN, glycine, alanine, citrulline, GABA, asparagine, methionine, serine, and hydroxyproline while KNO_3-fed plants were enriched in isoleucine and tyrosine (Figures 4D and S6A,B). These patterns align with Svietlova et al. (2024) who reported clear PCA separation between L-GLN and NO_3^- treatments. Although the most abundant amino acids differ between studies, likely due to growth conditions, N concentrations used, and developmental stage, both demonstrate N source-dependent shifts in overall amino acid profiles.

Despite these N source-driven differences, PCA analysis revealed that the overall amino acid variation was insufficient to clearly separate the mutant genotypes. Given the differential root growth responses to L-GLN and KNO_3 observed in mutants *chl1.10* and *amt qko* (Figure 4C), we therefore explored whether plant hormone regulation might underlie these phenotypes. Both auxin and cytokinin are known to play central roles in root development in response to KNO_3 (Asim et al. 2020) and L-GLN (Krouk et al. 2010; Liao et al. 2024).

Although overall auxin and cytokinin signaling in root tips did not differ significantly between KNO_3 and L-GLN (Figure 5A,B), hormone profiling revealed differences in absolute levels (Figure 6A,B), suggesting a link to the distinct root phenotypes associated with these N sources. The discrepancy between metabolite distribution and reporter-based activity may reflect localized changes in hormone distribution or signaling not captured by bulk analysis.

L-GLN-grown wild type plants had lower bioactive IAA levels and higher inactive metabolites (IAA-Glc, oxIAA and oxIAA-Glc; Figure 6A), indicating activation of auxin detoxification via oxidation and conjugation (Östin et al. 1998; Rampey et al. 2004; Porco et al. 2016). Such profiles often reflect feedback regulation in response to elevated local auxin (Novák et al. 2012; Ljung 2013), correlating with enhanced LR formation (Figure 2). These auxin patterns were largely similar across WT and the mutants, suggesting that they did not contribute to the differential L-GLN responses among genotypes. Instead, NRT1.1/CHL1, which regulates local auxin transport and tissue sensitivity in response to nitrate (Krouk et al. 2010; Mounier et al. 2013; Remans et al. 2006; Maghiaoui et al. 2020), likely modulates how this systemic hormonal environment is interpreted at the organ and tissue level, explaining why *chl1.10* shows altered root growth despite comparable whole-tissue hormone levels. L-GLN's promotion of LRs via repression of *IAA12* and *IAA14* and upregulation of *ARF5* (Liao et al. 2024), along with the restoration of root growth inhibition by auxin supplementation (Figure 5C), underscores auxin's key role in root development under L-GLN.

Cytokinin analysis revealed N source-specific regulation of biosynthesis (Figure 6B). While KNO_3 affects iP-cytokinin biosynthesis via *IPT3* (Wang et al. 2004), L-GLN promotes cZ-cytokinin accumulation likely through a distinct, KNO_3-independent pathway. Elevated cZ levels in L-GLN-grown WT plants may support root development, as cZ-deficient *ipt29* mutants exhibit strongly reduced root growth (Kiba et al. 2013). Conversely, the increased root biomass under L-GLN aligns with reduced tZ and iP levels, consistent with their inhibitory role in root development (Werner et al. 2003; Kieber and Schaller 2018). Importantly, mutants with enhanced root biomass under L-GLN (*amt tko, gogat*; Figure 4B,C) displayed decreased tZ levels, whereas mutants with reduced or no response (*chl1.10, gln tko*) maintained tZ levels, suggesting a link between tZ and L-GLN–mediated root growth. These patterns reflect the distinct functions of cytokinin types: impaired iP/tZ promotes root elongation, while cZ deficiency inhibits growth (Miyawaki et al. 2006; Kiba et al. 2013; Antoniadi et al. 2022), with tZ also influencing LR positioning (*CYP735A* mutants; Chang et al. 2015). This dual modulation of cytokinin types by L-GLN provides a mechanistic explanation for L-GLN–dependent root system architecture and demonstrates that organic N sources can directly shape hormone homeostasis.

In summary, our work reveals a central role for L-GLN in regulating root development in *Arabidopsis thaliana* through mechanisms distinct from KNO_3-dependent pathways, highlighting how N sources can drive root plasticity to optimize nutrient acquisition and utilization. For the first time, we demonstrate that L-GLN acts on low concentration levels even in the presence of high nitrate, suggesting its function not only as a nitrogen source but as an active signaling molecule capable of modulating RSA.

Phenotypically, L-GLN promotes LR formation, root hair development, higher-order branching, and overall root biomass.

The interplay between L-GLN transporters' activity, metabolic assimilation and hormonal regulation supports the regulatory capacity of L-GLN. AAP1-mediated uptake and GS-dependent assimilation are key to L-GLN-induced root biomass accumulation, while the contrasting responses to KNO_3 and L-GLN involve the canonical inorganic N sensors NRT1.1 and AMT—a connection not described before. At the hormonal level, L-GLN modulates auxin homeostasis to promote lateral root initiation, with auxin supplementation restoring primary root growth and LR symmetry. Additionally, L-GLN promotes previously unrecognized changes in cytokinin balance by elevating cZ to support elongation while reducing tZ to facilitate lateral root formation.

Together, these findings highlight L-GLN as an important integrator of N metabolism and hormone signaling in root development. This work provides a framework for future studies on organic N signaling and offers perspectives for improving N use efficiency, with potential applications in sustainable agricultural practices.

Author Contributions

K.L., I.A., and B.P. acquired the funding and conceptualized the study. B.P., A.I.J., M.J., I.A., and J.Š. performed experiments and data analysis. I.A. and B.P. prepared the figures and wrote the manuscript. All authors read and approved the manuscript.

Acknowledgements

Research in the Ljung group was funded by the Knut and Alice Wallenberg Foundation (KAW 2016.0352, KAW 2020.0240), the Swedish Research Council (VR 2018-04235, VR 2021-04938), Kempestiftelserna (JCK22-0023, JCK-2711, SMK21-0041 and JCK-1811). B.P. was further financially supported by Kungl. Skogs-och Lantbruksakademien (KSLA; GFS2022-0106) and I.A. by Magnus Bergvalls foundation (2021-04464). For access to instrumentation we thank the Swedish Metabolomics Centre (https://www.swedishmetabolomicscentre.se/), the UPSC Microscopy facility (https://www.upsc.se/platforms/microscopy-facility.html), the Biochemical Imaging Center at Umeå University, Irene Martinez Carrasco with the National Microscopy Infrastructure, NMI (VR-RFI 2019-00217) for providing assistance in microscopy and UPSC Growth Facility for technical support. Also, we thank Professors Céline Masclaux-Daubresse, Nicolaus von Wirén, Yi-Fang Tsay, Alain Gojon, June M. Kwak and Edward E. Farmer for sending seeds used in this work as well as Charikleia Nikolaou and Torgny Näsholm for critical reading of the manuscript. A generative AI tool (ChatGPT, OpenAI) was used to assist in improving the structure and clarity of the manuscript text. All scientific content, data interpretation, and conclusions were produced and verified by the authors.

Funding

This work was supported by Kempestiftelserna (JCK-1811, JCK-2711, JCK22-0023). Kungl. Skogsoch Lantbruksakademien (GFS2022-0106). Magnus Bergvalls Stiftelse (Stockholm, SE), (2021-04464). Knut and Alice Wallenberg Foundation (KAW 2016.0352, KAW 2020.0240). Vetenskapsrådet (VR 2018-04235, VR 2021-04938, VR-RFI 2019-00217).

Data Availability Statement

All data supporting the findings of this study are uploaded and can be accessed at https://www.upsc.se/karin_ljung under Supplemental Resources.

References

Aloni, R., E. Aloni, M. Langhans, and C. I. Ullrich. 2006. "Role of Cytokinin and Auxin in Shaping Root Architecture: Regulating Vascular Differentiation, Lateral Root Initiation, Root Apical Dominance and Root Gravitropism." *Annals of Botany* 97: 883–893.

Antoniadi, I., E. Mateo-Bonmatí, M. Pernisová, et al. 2022. "IPT9, a Cis-Zeatin Cytokinin Biosynthesis Gene, Promotes Root Growth." *Frontiers in Plant Science* 13: 9320.

Asim, M., Z. Ullah, F. Xu, et al. 2020. "Nitrate Signaling, Functions, and Regulation of Root System Architecture: Insights From *Arabidopsis thaliana*." *Genes* 11: 1–24.

Bielach, A., C. Cuesta, W. Grunewald, et al. 2012. "Spatiotemporal Regulation of Lateral Root Organogenesis in Arabidopsis by Cytokinin." *Plant Cell* 24: 3967–3981.

Cambui, C. A., H. Svennerstam, L. Gruffman, A. Nordin, U. Ganeteg, and T. Näsholm. 2011. "Patterns of Plant Biomass Partitioning Depend on Nitrogen Source." *PLoS One* 6: e19211.

Chang, L., E. Ramireddy, and T. Schmülling. 2015. "Cytokinin as a Positional Cue Regulating Lateral Root Spacing in Arabidopsis." *Journal of Experimental Botany* 66: 4759–4768.

Chen, L., and D. R. Bush. 1995. "LHT1, a Lysine- and Histidine-Specific Transporter in Arabidopsis." *Plant Physiology* 11: 11–27.

Coruzzi, G. M. 2003. "Primary N-Assimilation Into Amino Acids in Arabidopsis." *Arabidopsis Book* 2: e0010.

Coschigano, K. T., R. Melo-Oliveira, J. Lim, and G. M. Coruzzi. 1998. "Arabidopsis Gls Mutants and Distinct Fd-GOGAT Genes: Implications for Photorespiration and Primary Nitrogen Assimilation." *Plant Cell* 10: 741–752.

De Klerk, G. J. 1999. "The Formation of Adventitious Roots: New Concepts, New Possibilities." *In Vitro Cellular & Developmental Biology-Plant* 35: 189–199.

De Smet, I., S. Vanneste, D. Inzé, and T. Beeckman. 2006. "Lateral Root Initiation or the Birth of a New Meristem." *Plant Molecular Biology* 60: 871–887.

Duan, X., L. Luo, Z. Wang, et al. 2023. "Promotion of Root Development by Slightly Alkaline pH Involves an Auxin-Mediated Adaption Mechanism." *Soil Science and Environment* 2: 6.

El-Dawayati, M. M., H. S. Ghazzawy, and M. Munir. 2018. "Somatic Embryogenesis Enhancement of Date Palm Cultivar Sewi Using Polyamines and Glutamine Under Solid and Liquid Media Conditions." *International Journal of Biological Sciences* 12: 149–159.

Forsum, O., H. Svennerstam, U. Ganeteg, and T. Näsholm. 2008. "Capacities and Constraints of Amino Acid Utilization in Arabidopsis." *New Phytologist* 179: 1058–1069.

Ganeteg, U., I. Ahmad, S. Jämtgård, C. Aguetoni-Cambui, E. Inselsbacher, and H. Svennerstam. 2017. "Amino Acid Transporter Mutants of Arabidopsis Provide Evidence That a Non-Mycorrhizal Plant Acquires Organic Nitrogen From Agricultural Soil." *Plant and Soil* 40: 413–423.

Geiss, G., L. Gutierrez, and C. Bellini. 2009. "Adventitious Root Formation: New Insights and Perspectives." *Annual Plant Reviews* 37: 127–156.

Gilroy, S., and D. L. Jones. 2000. "Through Form to Function: Root Hair Development and Nutrient Uptake." *Trends in Plant Science* 5: 56–60.

Gioseffi, E., A. de Neergaard, and J. K. Schjoerring. 2012. "Interactions Between Uptake of Amino Acids and Inorganic Nitrogen in Wheat Plants." *Biogeosciences* 9: 1509–1518.

Gray, W. M. 2004. "Hormonal Regulation of Plant Growth and Development." *PLoS Biology* 2: e311.

Han, M., M. Xu, S. Wang, L. Wu, S. Sun, and T. Su. 2022. "Effects of Exogenous L-Glutamine as a Sole Nitrogen Source on Physiological Characteristics and Nitrogen Use Efficiency of Poplar." *Plant Physiology and Biochemistry* 172: 1–13.

Hassan, M. U., M. M. Islam, R. Wang, et al. 2020. "Glutamine Application Promotes Nitrogen and Biomass Accumulation in Maize Hybrid Seedlings." *Planta* 251: 66.

Hirner, A., F. Ladwig, H. Stransky, et al. 2006. "Arabidopsis LHT1 Is a High-Affinity Transporter for Cellular Amino Acid Uptake in Both Root Epidermis and Leaf Mesophyll." *Plant Cell* 18: 1931–1946.

Ho, C. H., S. H. Lin, H. C. Hu, and Y. F. Tsay. 2009. "CHL1 Functions as a Nitrate Sensor in Plants." *Cell* 18: 1184–1194.

Hodge, A., G. Berta, C. Doussan, F. Merchan, and M. Crespi. 2009. "Plant Root Growth, Architecture and Function." *Plant and Soil* 321: 153–187.

Hunt, E., S. Gattolin, H. J. Newbury, et al. 2010. "A Mutation in Amino Acid Permease AAP6 Reduces Amino Acid Content of Sieve Elements but Leaves Aphids Unaffected." *Journal of Experimental Botany* 61: 55–64.

Inselsbacher, E., and T. Näsholm. 2012. "The Below-Ground Perspective of Forest Plants: Soil Provides Mainly Organic Nitrogen for Plants and Mycorrhizal Fungi." *New Phytologist* 195: 329–334.

Jämtgård, S., T. Näsholm, and K. Huss-Danell. 2010. "Nitrogen Compounds in Soil Solutions of Agricultural Land." *Soil Biology and Biochemistry* 42: 2325–2330.

Javelle, A., M. Morel, B. R. Rodríguez-Pastrana, et al. 2003. "Molecular Characterization, Function and Regulation of Ammonium Transporters and Ammonium-Metabolizing Enzymes in Hebeloma Cylindrosporum." *Molecular Microbiology* 47: 411–430.

Kan, C. C., T. Y. Chung, Y. A. Juo, and M. H. Hsieh. 2015. "Glutamine Rapidly Induces Expression of Transcription Factors Involved in Nitrogen and Stress Responses in Rice Roots." *BMC Genomics* 16: 1–15.

Kiba, T., T. Kudo, M. Kojima, and H. Sakakibara. 2011. "Hormonal Control of Nitrogen Acquisition: Roles of Auxin, Abscisic Acid and Cytokinin." *Journal of Experimental Botany* 62: 1399–1409.

Kiba, T., K. Takei, M. Kojima, and H. Sakakibara. 2013. "Side-Chain Modification of Cytokinins Controls Shoot Growth in Arabidopsis." *Developmental Cell* 27: 452–461.

Kieber, J. J., and G. E. Schaller. 2018. "Cytokinin Signaling in Plant Development." *Development* 145: dev149344.

Kojima, S., H. Minagawa, C. Yoshida, E. Inoue, H. Takahashi, and K. Ishiyama. 2023. "Coregulation of GLN1;2 and GLT1 Expression in Arabidopsis Roots in Response to Ammonium." *Frontiers in Plant Science* 14: 1127006.

Kong, D., H. C. Hu, E. Okuma, et al. 2016. "L-Met Activates Arabidopsis GLR Ca2+ Channels Upstream of ROS and Regulates Stomatal Movement." *Cell Reports* 17: 2553–2561.

Krouk, G. 2017. "Nitrate Signalling: Calcium Bridges the Nitrate Gap." *Nature Plants* 3: 17095.

Krouk, G., B. Lacombe, A. Bielach, et al. 2010. "Nitrate-Regulated Auxin Transport by NRT1.1 Defines a Mechanism for Nutrient Sensing in Plants." *Developmental Cell* 18: 927–937.

Kudo, T., T. Kiba, and H. Sakakibara. 2010. "Metabolism and Long-Distance Translocation of Cytokinins." *Journal of Integrative Plant Biology* 52: 53–60.

Laplaze, L., E. Benková, I. Casimiro, et al. 2007. "Cytokinins Act Directly on Lateral Root Founder Cells to Inhibit Root Initiation." *Plant Cell* 19: 3889–3900.

Lardos, M., A. Marmagne, N. Bonadé Bottino, et al. 2023. "Discovery of the Biostimulant Effect of Asparagine and Glutamine on Plant Growth in Arabidopsis." *Frontiers in Plant Science* 14: 1281495.

Lavenus, J., T. Goh, I. Roberts, et al. 2013. "Lateral Root Development in Arabidopsis: Fifty Shades of Auxin." *Trends in Plant Science* 18: 450–458.

Lee, Y. H., J. Foster, J. Chen, L. M. Voll, A. P. M. Weber, and M. Tegeder. 2007. "AAP1 Transports Uncharged Amino Acids Into Arabidopsis Roots." *Plant Journal* 50: 305–319.

Liao, C. Y., W. Smet, G. Brunoud, S. Yoshida, T. Vernoux, and D. Weijers. 2015. "Reporters for Sensitive and Quantitative Measurement of Auxin Response." *Nature Methods* 12: 207–210.

Liao, H. S., K. T. Lee, Y. H. Chung, S. Z. Chen, Y. J. Hung, and M. H. Hsieh. 2024. "Glutamine Induces Lateral Root Initiation, Stress Responses and Disease Resistance in Arabidopsis." *Plant Physiology* 144: 2289–2308.

Lima, J. E., S. Kojima, H. Takahashi, and N. von Wirén. 2010. "Ammonium Triggers Lateral Root Branching in Arabidopsis in an AMT1;3-Dependent Manner." *Plant Cell* 22: 3621–3633.

Lipson, D., and T. Näsholm. 2001. "The Unexpected Versatility of Plants: Organic Nitrogen Use and Availability." *Oecologia* 128: 305–316.

Ljung, K. 2013. "Auxin Metabolism and Homeostasis During Plant Development." *Development* 140: 943–950.

Lonhienne, T. G. A., Y. Trusov, A. Young, et al. 2014. "Effects of Externally Supplied Protein on Root Morphology and Biomass Allocation in Arabidopsis." *Scientific Reports* 4: 5055.

López-Bucio, J., A. Cruz-Ramírez, and L. Herrera-Estrella. 2003. "The Role of Nutrient Availability in Regulating Root Architecture." *Current Opinion in Plant Biology* 6: 280–287.

Loqué, D., and N. von Wirén. 2004. "Regulatory Levels for the Transport of Ammonium in Plant Roots." *Journal of Experimental Botany* 55: 1293–1305.

MacGregor, D. R., K. I. Deak, P. A. Ingram, and J. E. Malamy. 2008. "Root System Architecture in Arabidopsis Grown in Culture Is Regulated by Sucrose Uptake in Aerial Tissues." *Plant Cell* 20: 2643–2660.

Maghiaoui, A., E. Bouguyon, C. Cuesta, et al. 2020. "NRT1.1 Coordinates Auxin Biosynthesis and Transport to Regulate Root Branching in Response to Nitrate." *Journal of Experimental Botany* 71: 4480–4494.

Meier, M., Y. Liu, K. S. Lay-Pruitt, H. Takahashi, and N. von Wirén. 2020. "Auxin-Mediated Root Branching Is Determined by Nitrogen Form." *Nature Plants* 6: 1136–1145.

Miflin, B. J., and D. Z. Habash. 2002. "The Role of Glutamine Synthetase and Glutamate Dehydrogenase in Nitrogen Assimilation." *Journal of Experimental Botany* 53: 979–987.

Miyawaki, K., P. Tarkowski, M. Matsumoto-Kitano, et al. 2006. "Roles of Arabidopsis ATP/ADP Isopentenyltransferases in Cytokinin Biosynthesis." *Proceedings of the National Academy of Sciences* 103: 16598–16603.

Moison, M., A. Marmagne, S. Dinant, et al. 2018. "Three Cytosolic Glutamine Synthetase Isoforms Act Together for N Remobilization and Seed Filling in Arabidopsis." *Journal of Experimental Botany* 69: 4379–4393.

Montiel, J., and J. G. Dubrovsky. 2024. "Amino Acid Biosynthesis in Root Hair Development: A Mini-Review." *Biochemical Society Transactions* 52: 1873–1883.

Mounier, E., M. Pervent, K. Ljung, A. Gojon, and P. Nacry. 2013. "Auxin-Mediated Nitrate Signalling by NRT1.1 in the Adaptive Response to Heterogeneous Nitrate Availability." *Plant, Cell & Environment* 37: 162–174.

Mousavi, S. A. R., A. Chauvin, F. Pascaud, S. Kellenberger, and E. E. Farmer. 2013. "Glutamate Receptor-Like Genes Mediate Leaf-To-Leaf Wound Signalling." *Nature* 500: 422–426.

Muños, S., C. Cazettes, C. Fizames, et al. 2004. "Transcript Profiling in the Chl1-5 Mutant of Arabidopsis Reveals a Role of the Nitrate Transporter NRT1.1 in the Regulation of Another Nitrate Transporter, NRT2.1." *Plant Cell* 16: 2433–2447.

Murashige, T., and F. Skoog. 1962. "A Revised Medium for Rapid Growth and Bioassays With Tobacco Tissue Cultures." *Physiologia Plantarum* 15: 473–497.

Nacry, P., E. Bouguyon, and A. Gojon. 2013. "Nitrogen Acquisition by Roots: Adaptation to Fluctuating Resources." *Plant and Soil* 370: 1–29.

Näsholm, T., K. Kielland, and U. Ganeteg. 2009. "Uptake of Organic Nitrogen by Plants." *New Phytologist* 182: 31–48.

Novák, O., E. Hényková, I. Sairanen, et al. 2012. "Tissue-Specific Profiling of the Arabidopsis Auxin Metabolome." *Plant Journal* 72: 523–536.

Ohkubo, Y., M. Tanaka, R. Tabata, M. Ogawa-Ohnishi, and Y. Matsubayashi. 2017. "Shoot-To-Root Mobile Polypeptides in Systemic Nitrogen Regulation." *Nature Plants* 3: 17029.

Östin, A., M. Kowalyczk, R. P. Bhalerao, and G. Sandberg. 1998. "Metabolism of IAA in Arabidopsis." *Plant Physiology* 118: 285–296.

Paungfoo-Lonhienne, C., T. G. A. Lonhienne, D. Rentsch, et al. 2008. "Plants Can Use Protein as a Nitrogen Source." *Proceedings of the National Academy of Sciences* 105: 4524–4529.

Pawar, B., P. Kale, J. Bahurupe, et al. 2015. "Proline and Glutamine Improve In Vitro Callus Induction and Shooting in Rice." *Rice Science* 22: 283–289.

Pedrotti, E. L., C. Jay-Allemand, P. Doumas, and D. Cornu. 1994. "Effect of Autoclaving Amino Acids on In Vitro Rooting of Wild Cherry." *Scientia Horticulturae* 57: 89–98.

Pěnčík, A., R. Casanova-Sáez, V. Pilarová, et al. 2018. "Ultra-Rapid Auxin Metabolite Profiling for High-Throughput Mutant Screening in Arabidopsis." *Journal of Experimental Botany* 69: 2569–2579.

Perchlik, M., J. Foster, and M. Tegeder. 2014. "Overlapping Functions of LHT6 and AAP1 in Root Amino Acid Uptake." *Journal of Experimental Botany* 65: 5193–5204.

Porco, S., A. Pěnčík, A. Rashed, et al. 2016. "AtDAO1 Controls IAA Oxidation and Homeostasis in Arabidopsis." *Proceedings of the National Academy of Sciences* 113: 11016–11021.

Rampey, R. A., S. LeClere, M. Kowalczyk, K. Ljung, G. Sandberg, and B. Bartel. 2004. "Auxin-Conjugate Hydrolases and Free IAA Levels During Germination." *Plant Physiology* 135: 978–988.

Ravelo-Ortega, G., J. S. López-Bucio, L. F. Ruiz-Herrera, et al. 2021. "Several Amino Acids Repress Arabidopsis Primary Root Growth Through Auxin-Dependent and Independent Mechanisms." *Plant Science* 302: 110–118.

Rawat, S. R., S. N. Silim, H. J. Kronzucker, M. Y. Siddiqi, and A. D. M. Glass. 1999. "AtAMT1 Expression and NH4+ Uptake Regulated by Glutamine Levels." *Plant Journal* 19: 143–152.

Remans, T., P. Nacry, M. Pervent, et al. 2006. "NRT1.1 in Nitrate-Rich Patch Signalling and Root Colonization." *Proceedings of the National Academy of Sciences* 103: 19206–19211.

Ristova, D., M. Giovannetti, K. Metesch, and W. Busch. 2016. "Natural Genetic Variation Shapes Root Responses to Phytohormones." *Plant Journal* 87: 76–90.

Riveras, E., J. M. Alvarez, E. A. Vidal, et al. 2015. "Calcium Is a Second Messenger in Nitrate Signalling." *Plant Physiology* 169: 1397–1404.

Ruffel, S., G. Krouk, D. Ristova, et al. 2011. "Nitrogen Economics of Root Foraging: Nitrate–Cytokinin Relay." *Proceedings of the National Academy of Sciences* 108: 18524–18529.

Sakakibara, H., K. Takei, and N. Hirose. 2006. "Interactions Between Nitrogen and Cytokinin in Metabolism." *Trends in Plant Science* 11: 440–448.

Sarropoulou, V. N., I. N. Therios, and K. N. Dimassi-Theriou. 2012. "Melatonin Promotes Adventitious Rooting in Sweet Cherry Rootstocks." *Journal of Pineal Research* 52: 38–46.

Schindelin, J., C. T. Rueden, M. C. Hiner, and K. W. Eliceiri. 2015. "The ImageJ Ecosystem." *Molecular Reproduction and Development* 82: 518–529.

Singh, S. K., C. T. Chien, and I. F. Chang. 2016. "GLR3.6 Controls Root Development via KRP4 Repression." *Journal of Experimental Botany* 67: 1853–1869.

Soldal, T., and P. Nissen. 1978. "Multiphasic Uptake of Amino Acids by Barley Roots." *Physiologia Plantarum* 43: 181–188.

Sun, C. H., J. Q. Yu, and D. G. Hu. 2017. "Nitrate: Crucial Signal in Lateral Root Development." *Frontiers in Plant Science* 8: 485.

Svačinová, J., O. Novák, L. Plačková, et al. 2012. "Miniaturized Cytokinin Purification Using Pipette Tip SPE." *Plant Methods* 8: 17.

Svennerstam, H., U. Ganeteg, C. Bellini, and T. Näsholm. 2007. "Mutant Screening Identifies LHT1 in Amino Acid Uptake." *Plant Physiology* 143: 1853–1860.

Svennerstam, H., U. Ganeteg, and T. Näsholm. 2008. "Uptake of Cationic Amino Acids Depends on AAP5." *New Phytologist* 180: 620–630.

Svennerstam, H., S. Jämtgård, I. Ahmad, et al. 2011. "Transporters Mediating Amino Acid Uptake at Natural Concentrations." *New Phytologist* 191: 459–467.

Svietlova, N., L. Zhyr, M. Reichelt, V. Grabe, and A. Mithöfer. 2024. "Glutamine Prevents NRT2.4 Induction and Affects Amino Acid Metabolism." *Frontiers in Plant Science* 15: 1369543.

Takahashi, F., K. Sato-Nara, K. Kobayashi, M. Suzuki, and H. Suzuki. 2003. "Sugar-Induced Adventitious Roots in Arabidopsis." *Journal of Plant Research* 116: 83–91.

Tünnermann, L., C. Aguetoni Cambui, O. Franklin, P. Merkel, T. Näsholm, and R. Gratz. 2025. "Plant Organic Nitrogen Nutrition: Costs, Benefits and Carbon Use Efficiency." *New Phytologist* 245: 1018–1028.

Van Norman, J. M., W. Xuan, T. Beeckman, and P. N. Benfey. 2013. "Pre-Patterning and Lateral Root Formation." *Development* 140: 4301–4310.

Vincill, E. D., A. E. Clarin, J. N. Molenda, and E. P. Spalding. 2013. "Glutamate Receptor-Like Proteins Regulate Lateral Root Initiation." *Plant Cell* 25: 1304–1313.

Walch-Liu, P., and B. G. Forde. 2008. "Nitrate Signalling via NRT1.1 Antagonizes L-Glutamate Effects." *Plant Journal* 54: 820–828.

Walch-Liu, P., I. I. Ivanov, S. Filleur, Y. Gan, T. Remans, and B. G. Forde. 2006. "Nitrogen Regulation of Root Branching." *Annals of Botany* 97: 875–881.

Wang, R., R. Tischner, R. A. Gutiérrez, et al. 2004. "Genomic Analysis of Nitrate Responses in a Nitrate Reductase-Null Arabidopsis Mutant." *Plant Physiology* 136: 2512–2522.

Wang, Y. Y., P. K. Hsu, and Y. F. Tsay. 2012. "Uptake, Allocation and Signalling of Nitrate." *Trends in Plant Science* 17: 458–467.

Werner, T., V. Motyka, V. Laucou, et al. 2003. "Cytokinin-Deficient Arabidopsis Plants Show Altered Shoot and Root Meristem Activity." *Plant Cell* 15: 2532–2550.

Yao, X., J. Nie, R. Bai, and X. Sui. 2020. "Amino Acid Transporters in Plants: Identification and Function." *Plants* 9: 972.

Yuan, L., D. Loqué, S. Kojima, et al. 2007. "Organization of High-Affinity Ammonium Uptake in Arabidopsis Depends on AMT1 Transporters." *Plant Cell* 19: 2636–2652.

Zhang, S., F. Peng, Y. Xiao, W. Wang, and X. Wu. 2020. "Peach PpSnRK1 Participates in Sucrose-Mediated Root Growth via Auxin Signalling." *Frontiers in Plant Science* 11: 409.

Zhao, L., F. Liu, N. M. Crawford, and Y. Wang. 2018. "Molecular Regulation of Nitrate Responses in Plants." *International Journal of Molecular Sciences* 19: 2039.

Zürcher, E., D. Tavor-Deslex, D. Lituiev, K. Enkeli, P. T. Tarr, and B. Müller. 2013. "A Synthetic Sensor to Monitor Transcriptional Output of Cytokinin Signalling." *Plant Physiology* 161: 1066–1075.

Zygalakis, K. C., T. Roose, and I. C. Dodd. 2011. "Modelling Root Hair Contribution to Nutrient Uptake." *Plant, Cell & Environment* 34: 1112–1124.

Supporting Information

Additional supporting information can be found online in the Supporting Information section. **Datat S1.** The complete LC–MS quantification and statistics of all amino acids evaluated in roots of all mutants grown in different N conditions. **Table S1:** List of primers. **Table S2:** MS conditions for quantitative amino acid analysis. **Table S3:** Differential root growth of various N-related mutants in response to organic and inorganic N. **Figure S1:** The effect of Arabidopsis genetic background on L-GLN response. **Figure S2:** Screening of various amino acids to identify the most effective root-promoting candidate. **Figure S3:** Effect of sucrose on the plant growth. **Figure S4:** Determining L-GLN specificity in root development. **Figure S5:** Dose response effect of ammonium and L-GLN treatments on plant growth. **Figure S6:** LC–MS quantification of amino acids in roots of plants grown in different N conditions. **Figure S7:** Feeding experiment with isotopically labelled GLN revealed distinct paths of GLN assimilation.